

Mars Reconnaissance Orbiter: Aerobraking Reference Trajectory

by

Daniel T. Lyons
California Institute of Technology
Jet Propulsion Laboratory
Daniel.T.Lyons@jpl.nasa.gov
(818) 393-1004

Abstract:

The Mars Reconnaissance Orbiter spacecraft will be launched between August 8 and August 28 on a Type 1 trajectory during the 2005 Mars launch opportunity. After propulsively capturing into a 35 hour highly elliptical orbit with a 300 km periapsis altitude, the spacecraft will undergo a checkout period before beginning a 6 month aerobraking phase. This paper describes the aerobraking baseline trajectory that formed the basis of the reference mission presented at the Mars Reconnaissance Orbiter Preliminary Design Review.

Introduction:

The Mars Reconnaissance Orbiter (MRO) will arrive at Mars between March 8 and March 28, 2006 and will be propulsively captured into a 35 hour highly elliptical capture orbit. The 93° inclination target at arrival is determined by the frozen, 3:15 pm mean local solar time sun-synchronous final mapping orbit. Rather than carry extra propellant to propulsively change the orbit node to reduce the time required for the ascending node to reach 3:15 pm, the desired mean local solar time will be achieved by the motion of Mars around the Sun, combined with the very slow average nodal drift during aerobraking. (Propulsive options to use unallocated propellant to reach the mapping orbit more rapidly will be studied later and might be used if a favorable injection provided sufficient unallocated propellant.) The 5 hour change in mean local solar time takes nearly 6 months.

The most dangerous aspect of aerobraking is the unpredictable variability of the atmospheric density. A sudden increase in density will lead to unexpectedly high temperatures on the exposed spacecraft surfaces. The atmospheric variability margin can be maximized by spreading the aerobraking phase evenly across the available six months required for the mean local solar time change. The large time available for aerobraking coupled with a relatively low spacecraft ballistic coefficient means that MRO will have more margin for atmospheric variability than any previous aerobraking mission.¹⁻¹⁴

Spacecraft Description:

Figure 1 shows the MRO spacecraft in the aerobraking configuration. Unlike previous aerobraking spacecraft with deployable antennas,⁹⁻¹⁴ the MRO high gain

antenna (HGA) will be deployed prior to the start of aerobraking and used as one of the drag surfaces. The other primary drag surfaces are the two solar arrays and the spacecraft bus. The velocity of the spacecraft relative to the atmosphere during a drag pass will be nearly aligned with the +Y axis of the spacecraft, since this attitude is such that the aerodynamic torques on the vehicle are zero. The +Z axis will be pointed toward nadir during the drag pass. The positions of the solar panels will be tweaked after observing the aerodynamic torques during the walkin phase to achieve a zero “rolling” moment about the velocity vector. The panels and HGA will be held in position against the aerodynamic bending torques on the gimbals by powering the gimbals during the drag pass. The Mars Global Surveyor (MGS)⁹⁻¹² had a hard gimbal stop for the aerobraking configuration, while the Odyssey mission¹³⁻¹⁴ “latched” the solar panel in a hook for the aerobraking configuration. Because the MGS spacecraft suffered damage during the solar panel deployment,¹⁰ one of the panels had to be held in place by powering the gimbal, so this powered gimbal approach has been proven in flight.

In order to minimize the chance of going through a drag pass in the wrong configuration, the aerobraking configuration will not be changed for the entire duration of the aerobraking phase. After each drag pass, the entire spacecraft will be reoriented to point the HGA at the Earth, like was done for the Magellan and MGS missions.⁹ Because the active sides of the solar arrays will be pointed in the same general direction as the HGA boresight, and because the Earth and Sun are close together as viewed from Mars during the aerobraking phase, adequate solar power will be available. The most power critical period during aerobraking is near the end, when the time available for recharging is small because the orbit period is small and the eclipse and off-Sun (drag attitude) durations are large.

The turns to and from the drag attitude will be performed using the reaction wheels to minimize propellant usage during the aerobraking phase. The turn to the drag attitude will begin early enough to achieve the desired attitude for entry at least 5 minutes before atmospheric entry to accommodate timing prediction errors introduced by the atmospheric variability. MRO plans to use autonomous timing updates¹⁶⁻¹⁹ to minimize the size of the timing errors while reducing the number of uploads required during aerobraking. MRO also plans to use the atmosphere to unload the two reaction wheels that are orthogonal to the velocity vector by spinning these wheels down while in the atmosphere each orbit such that the resulting aerodynamic moment will produce the external moment required to unload the wheels.¹⁸⁻¹⁹ The axis that is aligned with the velocity vector could be unloaded by introducing a slight “propeller like” configuration to the solar panels to provide an aerodynamic moment about the “roll” axis, however, this would require new flight software. Since flight software is extremely expensive, a more cost effective may be to unload the roll axis using propellant in the traditional manner.

The MRO spacecraft is being built at the Lockheed-Martin Astronautics facility in Denver Colorado.

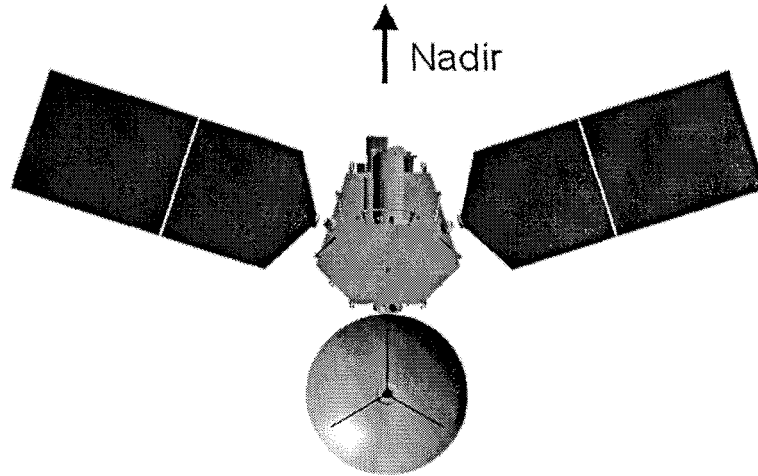


Figure 1: MRO in the Aerobraking Configuration as viewed Along Velocity Vector

Aerobraking Baseline Trajectory:

The periapsis altitude target for Mars Orbit Insertion (MOI) must be high enough above the atmosphere to accommodate navigation errors during approach to Mars. A 300 km periapsis target provides a reasonable balance between propulsive efficiency and safety during the propulsive capture into orbit at arrival. A southern approach is used because it maximizes the fraction of the MOI burn that is visible from the Earth so that some telemetry will be available in the event of a non-nominal insertion. The southern approach has the desirable property that periapsis tends to drift out of the atmosphere for most of the aerobraking phase, which minimizes risk in the event of a problem with the Deep Space Network (DSN) that prevents timely commanding of the spacecraft. The inclination changes by only a fraction of a degree during the aerobraking phase, so the capture orbit will be targeted close to the desired final value. The node is determined by the approach trajectory, which is primarily a function of the launch and arrival dates, which are chosen to minimize a combination of the launch C_3 and the arrival V -infinity. Although the node can be changed slightly by changing the arrival date, the optimum approach is to pick the date to minimize the delta- V required to capture into orbit and accept the resulting node as a starting point. Several days are allocated for spacecraft configuration and checkout following MOI.

Aerobraking begins with a series of propulsive “walk-in” maneuvers at apoapsis which lower the periapsis altitude from the initial 300 km periapsis altitude. The first maneuver lowers periapsis to an altitude of about 150 km. Several other progressively smaller maneuvers on succeeding orbits continue to lower periapsis until the desired dynamic pressure for aerobraking is achieved. The first maneuver is targeted to an altitude where drag should be observable for the least dense atmosphere but where damage is not possible even for the most dense atmosphere imaginable. The remainder of the walk-in maneuvers for the actual mission will be computed based on the difference between the observed density from the previous orbits and the atmospheric model. Several walk-in maneuvers are spread across several orbits in order to accommodate atmospheric uncertainty, as well as to accommodate maneuver execution errors and to

allow the spacecraft stability and sequencing to be checked out for gradually increasing dynamic pressures.

Figure 2 shows the periapsis altitude for the baseline trajectory for the open and close of the launch period. The aerobraking trajectories for the open and close are very similar in all respects, so most figures will only show the data for the open of the launch period. The periapsis altitude figure shows that the start of aerobraking for the close begins 8 days later because arrival at the close is 8 days later than for the open of the launch period. The aerobraking altitude depends on the specific atmospheric model used in the simulation. The baseline was computed using MarsGRAM 2000 with the input parameters specified in the MRO Planetary Constants and Models Document.¹⁵

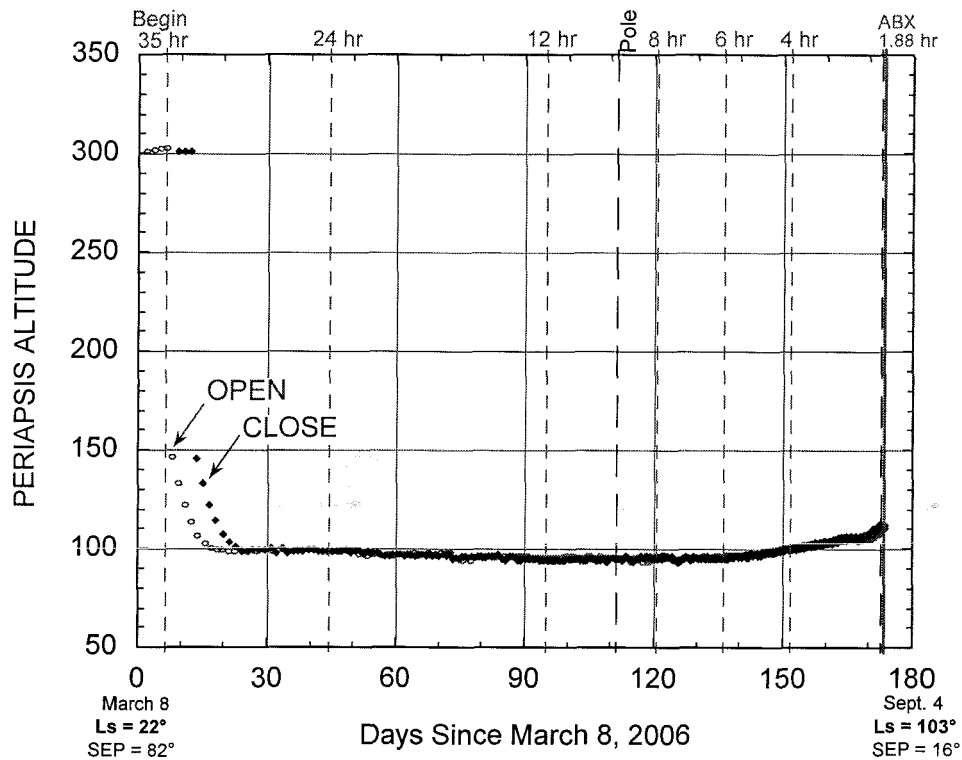


Figure 2: Periapsis Altitude for Open and Close of the Launch Period

During the course of aerobraking, gravitational asymmetries will precess the location of periapsis from an initial longitude of 70° S down across the South Pole, and then up across the equator. The location at closest approach to the South Pole and at the equatorial crossing are shown by vertical long-dashed lines at Day 110 and ABX. The short-dashed vertical lines show the orbit periods at various points for the open case, including the start of aerobraking and aerobraking exit (ABX). Since MarsGRAM models the effects of latitude and Solar illumination and season, the periapsis altitude must be forced down to lower altitudes as periapsis approaches the South pole, which is deep in winter, and must be allowed to drift higher when periapsis moves northward. Because periapsis tends to drift upward as periapsis precesses northward, no walkout maneuvers were required to raise periapsis to maintain a 2 day orbit lifetime. Once the

apoapsis reached an altitude of about 1000 km, periapsis was allowed to drift upward naturally such that the trajectory still had an orbit lifetime greater than two days when apoapsis reached the target value of 450 km. The baseline propellant budget is based on propulsively transferring to the mapping orbit once apoapsis reaches 450 km, although there is no technical reason that apoapsis could not be allowed to decay further in order to save additional propellant. The mapping orbit is a frozen, Sun-synchronous 320 x 255 km orbit with periapsis located at the South Pole.

Table 1: Key Simulation Parameters

Parameter	Value	
Mass	1225 kg	
Total Projected Area	36 m ²	
Drag Coef., C _D	2.2	
Ballistic Coefficient	15.5 kg/m ² (MGS was 22 kg/m ²)	
Atmosphere Model	MarsGRAM 2000	
Gravity Model	MGS85F2.GRV	
Gravity Field used in Simulation	12 x 12	
	OPEN	CLOSE
Launch Date	August 8, 2005	August 28, 2005
Arrival Date	March 8, 2006	March 16, 2006
Upper Dynamic Pressure Threshold	0.30 N/m ²	0.33 / 0.31 N/m ²
Lower Dynamic Pressure Threshold	0.19 N/m ²	0.22 / 0.19 N/m ²
Average Dynamic Pressure	0.23 N/m ²	0.23 N/m ²
Number of Aero Orbits Required	481 Orbits	470 Orbits
Number of Aero Days Required	166 Days	159 Days
Average Qdot (at Periapsis)	0.10 W/cm ²	0.10 W/cm ²
Maximum Simulated Qdot	0.16 W/cm ²	0.16 W/cm ²
Orbit Period (Start-End)	35 – 1.88 hours	
Ls (Start-End)	22° - 103°	
Sun-Earth-Probe Angle (Start-End)	82° - 16°	
One Way Light Time (Start-End)	12 – 21.5 minutes	
Eclipse (minimum – maximum)	11 – 37 minutes	
Occultation (minimum – maximum)	11 – 34 minutes	

Figure 3 shows the dynamic pressure for the baseline aerobraking trajectory for the Open of the launch period. I like to use a dynamic pressure corridor to design the

aerobraking trajectory because maintaining a constant dynamic pressure leads to a decreasing aerodynamic heat flux (Q_{dot}) at the end of aerobraking. Usually the thermal analysts require a lower Q_{dot} near the end of aerobraking because the duration of the aerodynamic heating pulse increases as the orbit becomes more circular, so the integrated heating becomes more of a factor. Since MRO is early in its project cycle, the dynamic pressure is being used as the design parameter in order to generate a baseline trajectory for the thermal analysts to analyze. The baseline trajectory supplies the aerodynamic heating directly, and also supplies the geometry needed to compute solar heating, planet albedo, and eclipse entry and exit. The solid black lines at 0.306 and 0.190 N/m^2 represent the corridor limits for this example. Some points lie outside the corridor because the simulation software only triggers a maneuver to raise or lower periapsis after the control corridor is exceeded. Note that the apparent randomness in the dynamic pressure points shown in Figure 3 are only due to variations due to gravitational perturbations that slightly raise or lower periapsis from orbit to orbit. The density from the MarsGRAM 2000 atmosphere model is the average value, and does not include any short term variability. Since the 1-sigma variability of the Mars atmosphere is known to be approximately 33%, a plot of the actual dynamic pressures would show a much larger range of values, and include many more points outside of the corridor limits that are used to trigger maneuvers in the simulation. Deciding when and how to perform corridor control maneuvers during flight is a much more interesting and challenging task than triggering maneuvers in a simulation!

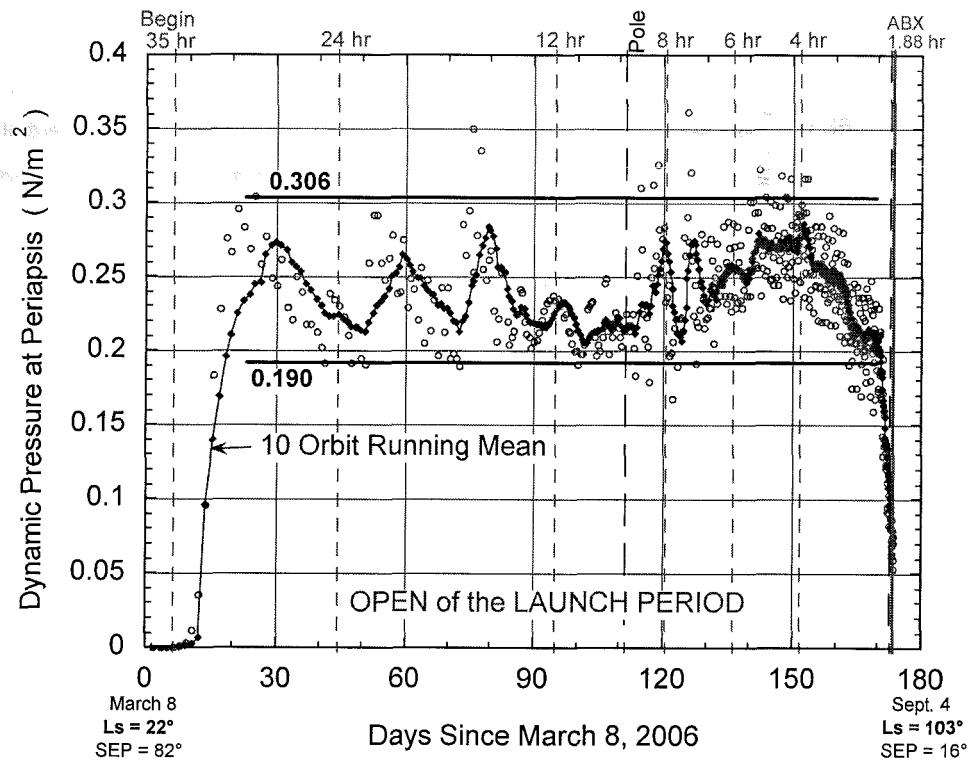


Figure 3: Dynamic Pressure at Periapsis

For these early trajectory designs, a constant dynamic pressure corridor of fixed width is increased or decreased in order to achieve the desired final 3:15 pm mean local

solar time target orbit conditions regardless of the resulting heating rates. These heating rates will then be compared to the limits that will eventually be established by the thermal analysts so that the next set of aerobraking trajectories can be modified to maximize the minimum margin. For the MRO mission, the heating rate margins are expected to be very large, as explained next.

The aerodynamic heating rate ($\dot{Q} = \frac{1}{2} \rho \cdot V^3$) is shown in Figure 4. The upper limit of the plot (0.7 W/cm^2) has been set equal to the upper limit for the Odyssey mission (the \dot{Q} where the predicted panel temperature²⁰ was equal to 175°C). If the upper temperature limit for MRO is the same as for Odyssey, and the flow field and heat transfer factors are also similar to those for Odyssey, then the current MRO mission has more than 300% margin relative to atmospheric variability! (For MGS, the \dot{Q} limit was 0.79 W/cm^2 .) Although this margin seems large enough to handle a daily orbit-to-orbit variability of 100% 3-sigma, Mars Global Circulation Model (MGCM) simulations suggest that the density can increase by a factor of 10 in only a few days if a global dust storm begins suddenly and is preceded by dust free atmospheric conditions. Thus, the flight team will have to continuously monitor the atmospheric conditions during aerobraking. Fortunately Mars is at aphelion during the MRO aerobraking phase, where the chance of a global dust storm is a minimum.

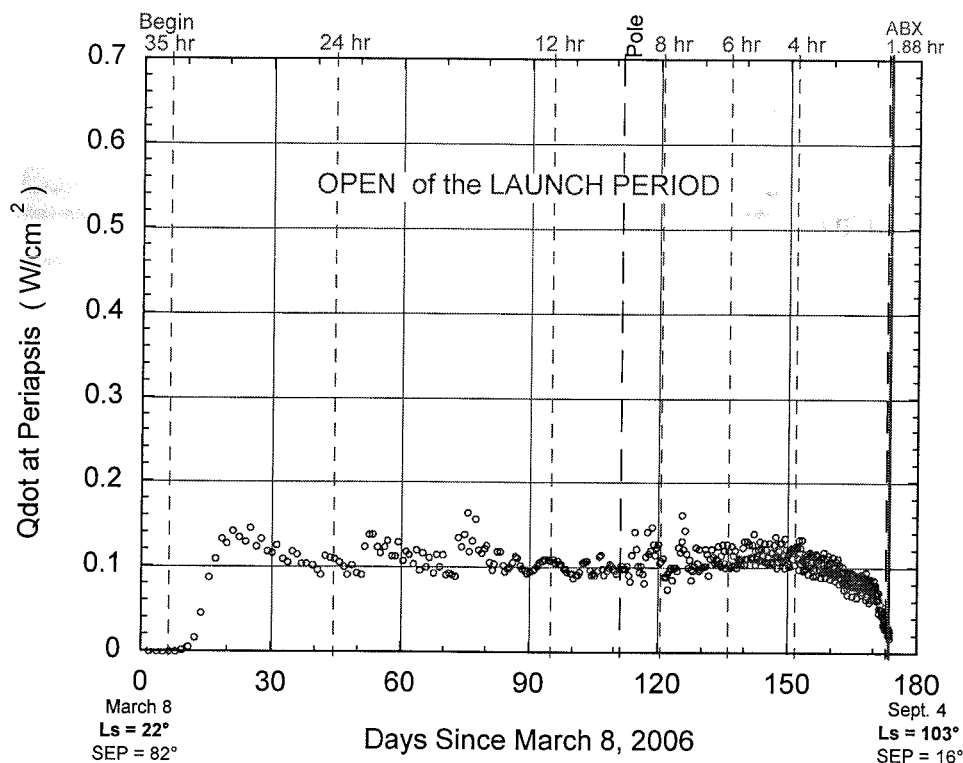


Figure 4: Qdot at Periapsis

Both the Dynamic Pressure and \dot{Q} are computed at periapsis by the “vpohop” simulation software which was developed for aerobraking Magellan at Venus. The periapsis values were very close to the maximum values at Venus, because Venus is a very round planet. The atmosphere model for Venus was not sufficiently well known to

include latitudinal effects. On the other hand, Mars has a significant bulge near the equator so that even with a purely exponential atmosphere, the maximum values of dynamic pressure and \dot{q} do not occur exactly at periapsis, but are biased toward the equator. The MarsGRAM atmosphere model is sophisticated enough to include latitudinal effects, including the lower temperatures and densities over the winter pole. Thus the maximum value of \dot{q} is usually a few percent larger than the value at periapsis shown in the plot, even with the “smooth” atmosphere provided by MarsGRAM. Accelerometer data from previous missions shows that on average the maximum deceleration is definitely offset from periapsis in the direction of the equator, but it also shows that waves in the atmosphere introduce a moderate amount of “noise” in the exact location of the peak.

A final note on the corridor is that for the close of the launch period case, the corridor was reduced toward the end of aerobraking to fine tune the final mean local solar time. Thus two different corridor zones were used, in addition to a “no corridor” at the start and end of aerobraking for the walk-in and walk-out phases. The somewhat chaotic interaction between the corridor limits, the maneuver sizes, and the gravity field can lead to some counter intuitive changes in the mean local solar time at the end. For example, increasing the dynamic pressure corridor thresholds should result in more drag per orbit on average resulting in a shorter aerobraking phase and thus a larger mean local solar time at the end, since the mean local solar time is decreasing as Mars moves around the Sun. Figure 5 shows that the rate of nodal precession increases as the apoapsis altitude becomes smaller, and eventually the nodal precession rate becomes large enough to achieve a Sun synchronous orbit, as shown in Figure 6, where the mean local solar time stops decreasing at the end of the aerobraking phase. A small increase in the corridor limits can result in a trajectory where periapsis spends more time near the lower limit, and thus lowers the average dynamic pressure for that case rather than increasing it. When a single corridor is used for the entire aerobraking phase, small increases in the corridor limits can result in small decreases, rather than small increases in the final mean local solar time. To further compound this effect, small changes in the corridor change the evolution of the orbit period, which changes the longitude of periapsis from one case to another. Periapsis altitude perturbations are primarily determined by the Longitude of periapsis. The inclination perturbation is also determined by the Longitude of periapsis, but the effect usually cancels out except near the resonance points (Figure 7). The inclination of a highly inclined orbit can increase or decrease rapidly near a resonance point due to the “sideways” force of bulges in the planet at Tharsis (Olympus Mons) and an apparent bulge on the other side of the planet. These effects can make it very difficult to find a single corridor definition that hits a specific final mean local solar time precisely. If a trajectory design has a mean local solar time that is only a few tenths of an hour too large, defining a second corridor with slightly lower limits for the latter part of the aerobraking phase makes it easier to tweak the final mean local solar time slightly. (The alternative of increasing the design corridor limits slightly near the end to increase the final mean local solar time slightly would normally not be recommended, since the thermal limits usually decrease as the drag duration increases.)

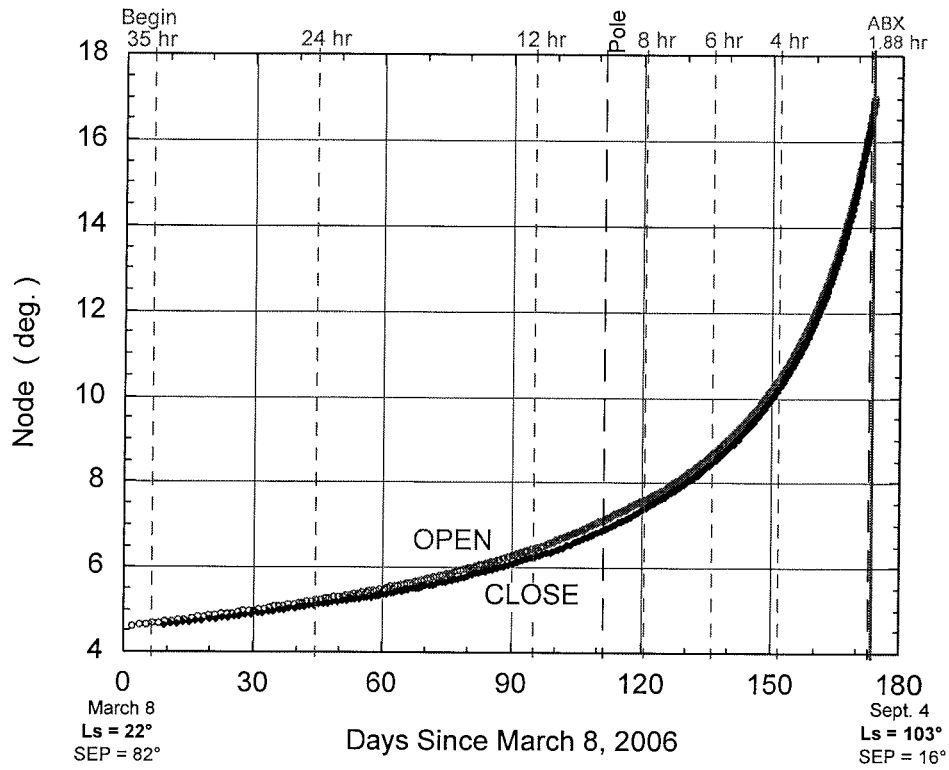


Figure 5: Node during Aerobraking

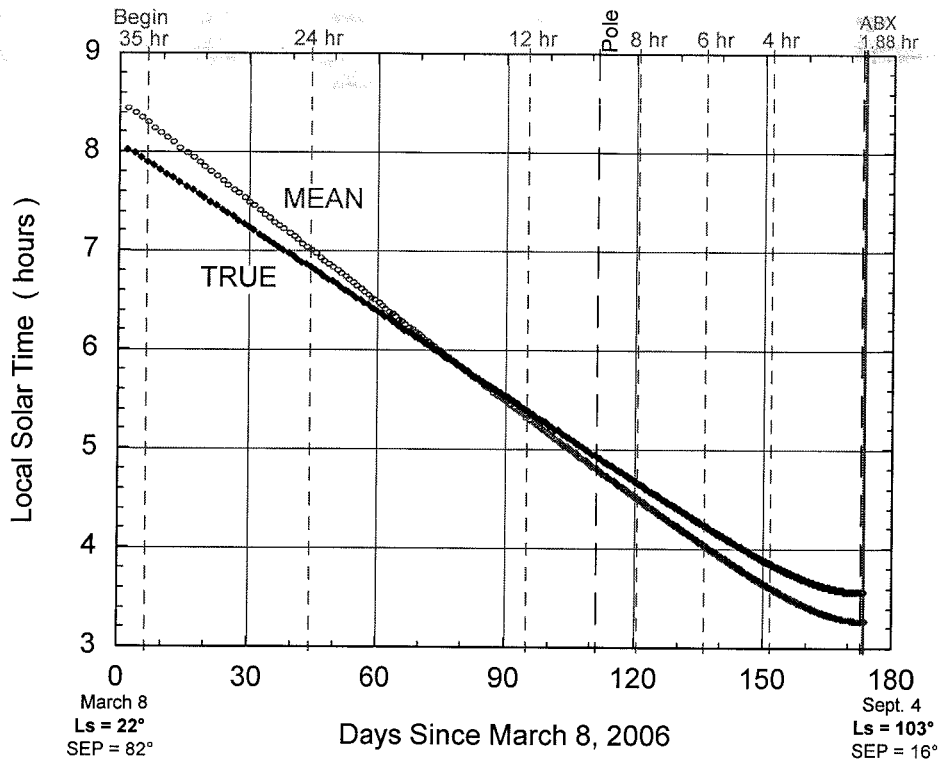


Figure 6: Mean Local Solar Time during Aerobraking.

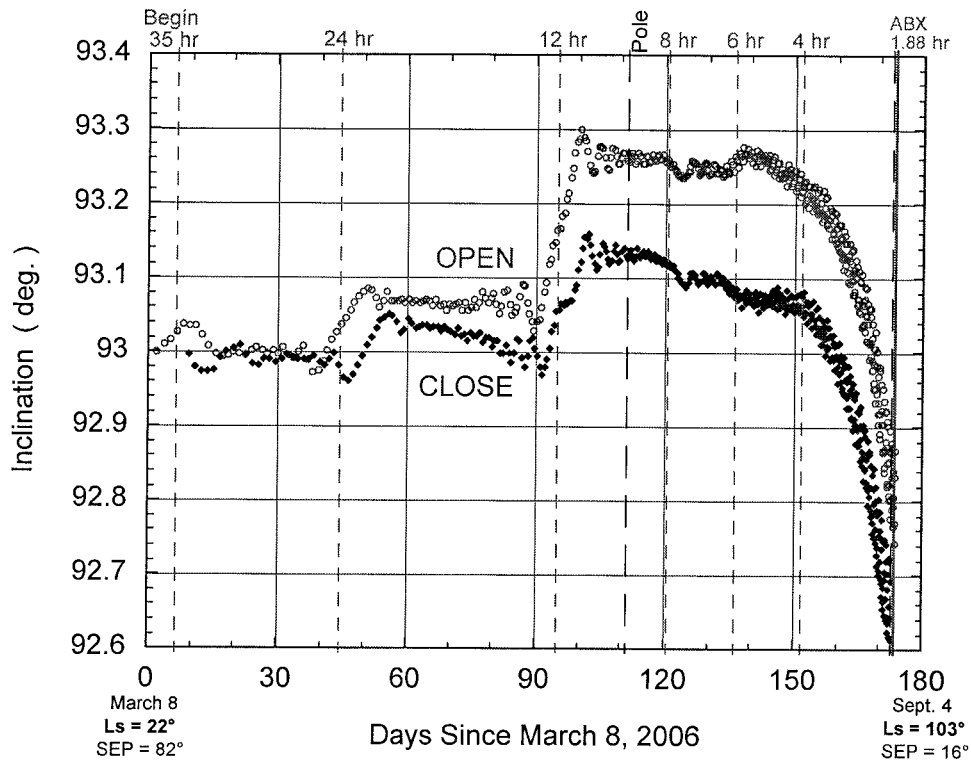


Figure 7: Inclination for Open and Close

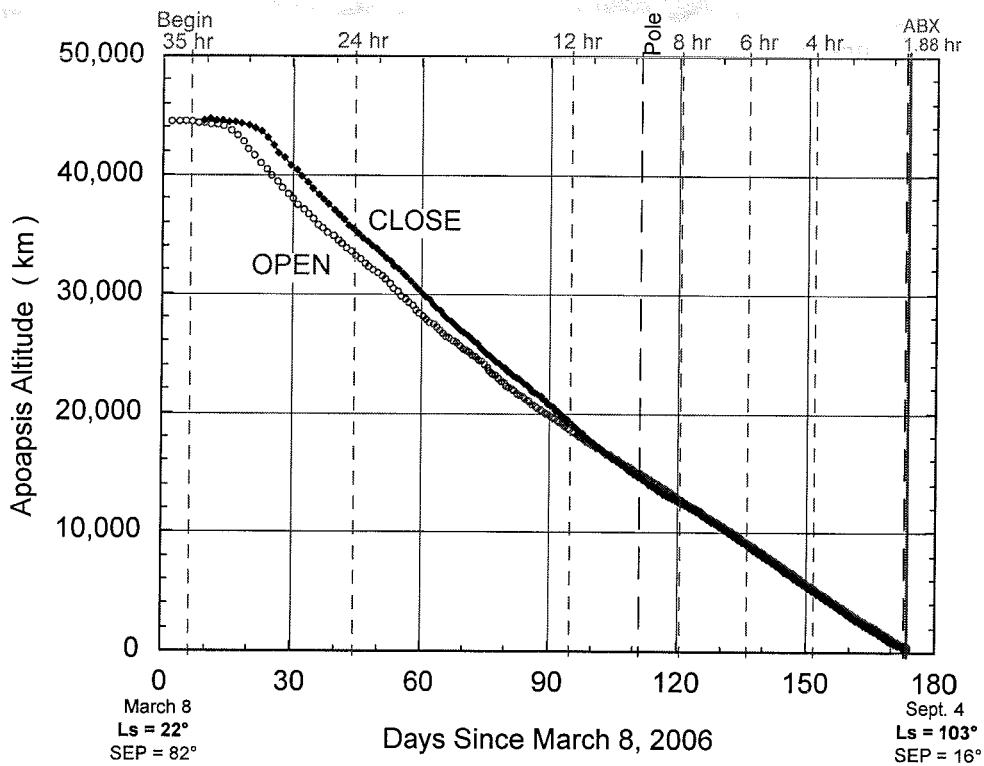


Figure 8: Apoapsis Altitude for Open and Close

Figure 8 shows the apoapsis altitude during the aerobraking phase. Maintaining a constant dynamic pressure corridor results in a nearly constant rate of apoapsis decay during the main phase of aerobraking. Decreasing the dynamic pressure at the end of aerobraking during the “walk-out” phase results in a steady reduction in the rate of apoapsis decay.

As mentioned earlier, the power balance near the end of aerobraking is usually an issue. As the orbit period shrinks, less and less time is available for recharging the batteries. The final orbit period at aerobraking exit (ABX) is only 113 minutes. The duration of the drag pass at ABX is 18 minutes. A conservative approach is to assume that no solar power is available while in the drag attitude, because this attitude is specified by the atmospheric relative velocity. If the spacecraft remains in the drag attitude for an additional 5 minutes on both sides of the drag pass, then the total time in the drag attitude is 28 minutes. Since it takes another 5 to 7 minutes to turn from the drag attitude to the Earth/Sun pointing attitude the total off Sun time due to the drag pass is about 40 minutes. Since MRO is targeted to a 3:15 mean local solar time, the eclipse duration at ABX is 37 minutes. If the drag pass and the eclipse do not overlap, only 46 minutes would be available for recharging the batteries each orbit. Fortunately, Figure 9 shows that there is almost complete overlap between the eclipse and the drag attitude at ABX, which means that 63 minutes out of the 113 minute final orbit period is available for charging the batteries. Unfortunately, periapsis in eclipse means that the velocity at apoapsis will be nearly orthogonal to the Sun, so propulsive corridor control maneuvers to raise and lower periapsis will be poorly oriented to collect power. Near the end of aerobraking, several orbits might be required after each propulsive maneuver to get the batteries back to a full state of charge.

Conclusions:

The aerobraking trajectory described in this paper provides the reference that was used to evaluate the spacecraft subsystems at the project Preliminary Design Review. The reference trajectory may change due to inputs from the spacecraft subsystems, or due to a project decision to trade margin for other project goals. The Mars Reconnaissance Orbiter aerobraking baseline described in this paper has more margin for atmospheric variability than any previous aerobraking mission. The margin is still not large enough to accommodate the order of magnitude change that the global circulation models say are possible during the start of a global dust storm, so the operations team will still have to closely monitor the atmospheric conditions during aerobraking. Because the planned duration of aerobraking is so large, automation will be used to reduce the number of uploads that are required to keep the spacecraft sequence in synch with reality.

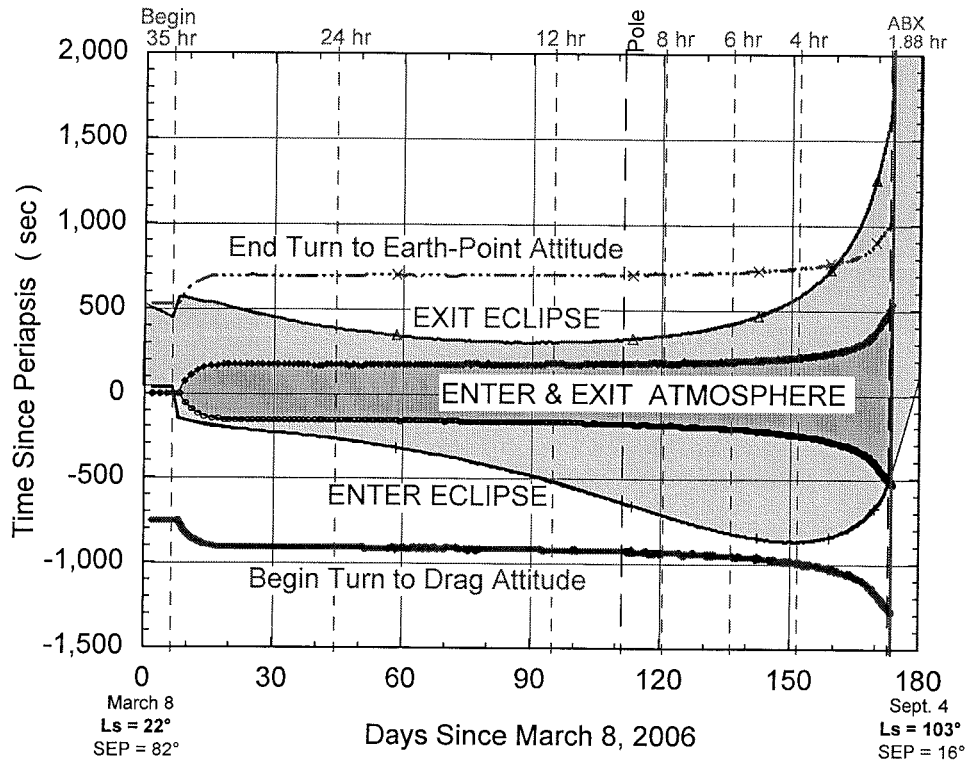


Figure 9: Eclipse and Atmospheric Entry and Exit

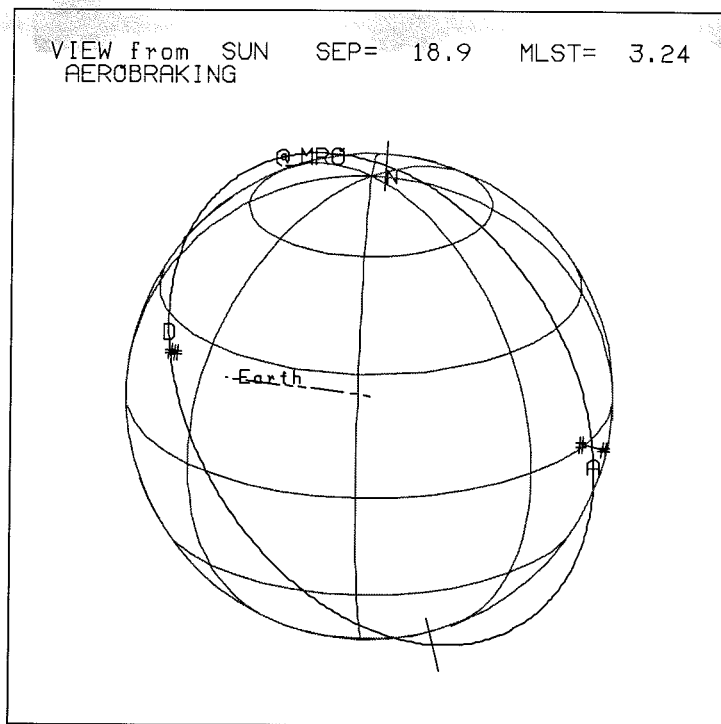


Figure 10: View of the Orbit just prior to Aerobraking Exit (ABX)

Acknowledgements:

The work described was performed at the Jet Propulsion Laboratory (JPL), California Institute of Technology under contract with the National Aeronautics and Space Administration (NASA).

References:

- ¹ D.T. Lyons, W. Sjogren, W.T.K. Johnson, D. Schmitt, and A. McRonald, "Aerobraking Magellan", AAS/AIAA Astronautics Conference, August 19-22, 1991, Durango Colorado. Paper AAS-91-420.
- ² D.T. Lyons, "Aerobraking Magellan: Plan versus Reality", AAS/AIAA Spaceflight Mechanics Meeting, Cocoa Beach Florida, February 14-16, 1994. Paper AAS 94-118.
- ³ D.T. Lyons, R. Stephen Saunders, and Douglas Griffith, "The Magellan Venus Mapping Mission: Aerobraking Operations", 44th Congress of the International Astronautical Federation, Graz, Austria, October 16-22, 1993. Paper IAF-93-Q.4.409.
- ⁴ R. Cook and D.T. Lyons, "Magellan Periapsis Corridor Design", AAS/AIAA Space Flight Mechanics Conference, Colorado Springs, Colorado. February 24-26, 1992. Paper AAS-92-159.
- ⁵ W.H. Willcockson, "Magellan Aerobraking Control Corridor Design & Implementation", AAS/AIAA Spaceflight Mechanics Meeting, Cocoa Beach Florida, February 14-16, 1994. Paper AAS 94-117.
- ⁶ A. Carpenter and E. Dukes, "Control of the Magellan Spacecraft During Atmospheric Drag", 17th annual AAS Guidance and Control Conference, Keystone Colorado, February 2-6, 1994. Paper AAS-94-064.
- ⁷ H. Curtis, "Reconstructing Time of Periapsis from Spacecraft Telemetry during Magellan Aerobraking", 17th annual AAS Guidance and Control Conference, Keystone Colorado, February 2-6, 1994. Paper AAS-94-054.
- ⁸ S.K. Wong, T-H. You, J.D. Giorgini, L. Lim, P. Chadbourne, "Navigating through the Venus Atmosphere", AAS/AIAA Spaceflight Mechanics Meeting, Cocoa Beach Florida, February 14-16, 1994. Paper AAS 94-116.
- ⁹ D.T. Lyons, "Aerobraking at Venus and Mars: A Comparison of the Magellan and Mars Global Surveyor Aerobraking Phases", AAS/AIAA Astrodynamics Conference, Girdwood Alaska, 16-19 August 1999. Paper AAS 99-358.
- ¹⁰ D.T. Lyons, "Mars Global Surveyor: Aerobraking with a Broken Wing", AIAA/AAS Astrodynamics Conference, Sun Valley Idaho, August 4-7, 1997. AAS-97-618.
- ¹¹ M.D. Johnston, et.al. "Mars Global Surveyor: Aerobraking at Mars", AAS/AIAA Space Flight Mechanics Meeting, Monterey, CA, Feb. 9-11, 1998. AAS 98-112.
- ¹² D.T. Lyons, J.G. Beerer, .P.B. Esposito, M.D. Johnston, W.H. Willcockson, "Mars Global Surveyor: Aerobraking Mission Overview", *Journal of Spacecraft and Rockets*, Volume 36, Number 3, May-June 1999. pp. 307-313.
- ¹³ J.C. Smith, J. Bell, "2001 Mars Odyssey Aerobraking", AIAA/AAS Astrodynamics Conference, Monterey CA, August 5-8, 2002. AIAA-2002-4532.
- ¹⁴ R. Mase, P. Antreasian, J. Bell, T. Martin-Mur and J. Smith, "The Mars Odyssey Navigation Experience", AIAA/AAS Astrodynamics Conference, Monterey CA, August 5-8, 2002. AIAA-2002-4530.
- ¹⁵ D. Highsmith, "Mars Reconnaissance Orbiter Project Planetary Constants and Models", JPL D-22685, May 17, 2002.

¹⁶ J. Hanna, R.H. Tolson, "An Approach for Autonomous Aerobraking to Mars", AIAA/AAS Astrodynamics Specialist Conference, Quebec City, Quebec, Canada, July 30-August 2, 2001, AAS-01-387

¹⁷ D.T. Lyons, "Aerobraking Automation Options", AIAA/AAS Astrodynamics Specialist Conference, Quebec City, Quebec, Canada, July 30-August 2, 2001, AAS-01-385

¹⁸ W.R. Johnson, J.M. Longuski, D.T. Lyons, "Attitude Control During Autonomous Aerobraking for Near-Term Mars Exploration", AIAA/AAS Astrodynamics Specialist Conference, Quebec City, Quebec, Canada, July 30-August 2, 2001, AAS-01-388

¹⁹ W.R. Johnson, J.M. Longuski, D.T. Lyons, "High-Fidelity Modeling of Semi-Autonomous Attitude Control During Aerobraking", AIAA/AAS Astrodynamics Specialist Conference, Quebec City, Quebec, Canada, July 30-August 2, 2001, AIAA-2002-4909.

²⁰ J. Dec, J. Gasbarre, "Thermal Modeling of the Mars Odyssey Solar Array – Lessons Learned", part of a presentation by NASA Langley to the Mars Reconnaissance Orbiter project, April 25, 2002.

AIAA-2002-4821